

## Surface oxidation of monodisperse SnO<sub>x</sub> nanoparticles

R. Ramamoorthy<sup>a,b</sup>, M.K. Kennedy<sup>a</sup>, H. Nienhaus<sup>b,\*</sup>,  
A. Lorke<sup>b</sup>, F.E. Kruis<sup>a</sup>, H. Fissan<sup>a</sup>

<sup>a</sup>Process- and Aerosol Measurement Technology, Gerhard-Mercator-Universität Duisburg, Bismarckstr. 81,  
D-47057 Duisburg, Germany

<sup>b</sup>Institute of Physics, Gerhard-Mercator-Universität Duisburg, Lotharstr.1,  
D-47048 Duisburg, Germany

Received 23 May 2002; accepted 8 October 2002

### Abstract

Monodisperse tin oxide nanoparticles of size from 10 to 25 nm with different initial oxygen stoichiometry are prepared by a gas-phase condensation technique. Auger electron spectroscopy is used to study the stoichiometric changes of the particle surfaces processed under different conditions. Annealing the as-deposited SnO<sub>x</sub> particles at 300 °C for 1 h in synthetic air leads to an intermediate phase of tin oxide and on further annealing, an equilibrium phase is stabilized. The annealing treatments oxidize the particle surface nearly to stoichiometric SnO<sub>2</sub>, depending on the initial oxygen content. In the case of pre-oxidized particles in the gas phase, an under-stoichiometric phase, with the surface composition of SnO<sub>1.8</sub>, is observed even after multiple heat treatments whereas the SnO particles, that are not pre-oxidized, transform into SnO<sub>2</sub> after annealing twice at 300 °C. The surface stoichiometry is not found to change with the particle size.

© 2002 Elsevier Science B.V. All rights reserved.

**Keywords:** Gas sensors; Tin oxide nanoparticles; Oxidation; Oxygen stoichiometry; Auger electron spectroscopy

### 1. Introduction

Tin oxide (SnO<sub>x</sub>)-based gas sensors have become important solid state devices for detecting combustible and toxic gases in the past few decades [1]. In recent years, the use of nanocrystalline particles with a high surface-to-volume ratio made it possible to improve the gas-sensing properties [2] which are mainly influenced by the surface region of the particles. Therefore, the study of surface/interface conductivity and geometric effects [3], of work function [4], microstructure [5] and the analysis of surface stoichiometry is of great importance to better understand the gas-sensing mechanism. The oxygen stoichiometry of tin oxide particles/surfaces varies between SnO and SnO<sub>2</sub> for different preparation and processing conditions. Since the charge transfer process is different in SnO and SnO<sub>2</sub>, the stoichiometric changes during synthesis need to be optimized and a stable stoichiometry must be formed for optimum sensor operation.

Oxidation of Sn and SnO thin films prepared by different techniques, from Sn and SnO<sub>2</sub> precursors, has been studied

by X-ray and ultraviolet photoelectron spectroscopy (XPS, UPS) and Rutherford backscattering spectroscopy (RBS) for many years [6,7]. Since no significant chemical shift between the Sn<sup>2+</sup> and Sn<sup>4+</sup> states can be detected by XPS, this method does not allow to identify the stoichiometric changes in SnO<sub>x</sub>.

Post-annealing treatments of Sn films at 450–550 °C for 4 h is found to oxidize the film to SnO<sub>1.85</sub> in air and to SnO<sub>2</sub> in oxygen [7]. However there is a strong dependence on the initial processing conditions of the films. In spite of many studies on the oxidation of SnO<sub>x</sub> thin films prepared from Sn or SnO<sub>2</sub> precursors, there is little amount of work on the oxidation process of SnO nanoparticles found in the literature.

It is well known that oxygen stoichiometry, annealing treatments and microstructure influence the sensitivity of SnO<sub>2</sub> thin film gas sensors [8]. Similar effects are expected with SnO<sub>x</sub> nanoparticle sensors. The present Auger electron spectroscopy (AES) study is thus focussed on variations of the initial surface stoichiometry of SnO and SnO<sub>x</sub>, (1 < x ≤ 2), nanoparticles prepared under different conditions and deposited onto a small circular spot (1–2 mm) on Si substrates. In addition, the change of surface composition after various annealing steps at 300 °C is investigated.

\* Corresponding author. Tel.: +49-203-379-3154;

fax: +49-203-379-2709.

E-mail address: [nienhaus@uni-duisburg.de](mailto:nienhaus@uni-duisburg.de) (H. Nienhaus).

## 2. Experiment

SnO nanoparticles with diameters of 10, 15, 20 and 25 nm are prepared by a gas-phase condensation method [9]. SnO powder (99%, Aldrich, Germany) is evaporated at  $(800 \pm 10)^\circ\text{C}$  in a tube furnace in nitrogen atmosphere. The SnO vapor condenses into particles which are transported to the deposition chamber by the carrier gas  $\text{N}_2$  at a constant flow rate of 1.6 l/min. Before deposition, the aerosol is charged by a radioactive neutralizer ( $\text{Kr}^{85}$ ). The

charged aerosol particles are then size-selected by a differential mobility analyser (DMA).

The size-selected particles are sintered inflight at  $650^\circ\text{C}$  for recrystallization and shape refinement in another furnace on their way to the deposition chamber. A schematic diagram of the experimental setup for preparation of the monodispersed nanoparticles is shown in Fig. 1(a). The particle concentration in the flow is monitored by a condensation nucleus counter (3025-TSI, Minneapolis, USA) and is dependent on the evaporation temperature [10]. For

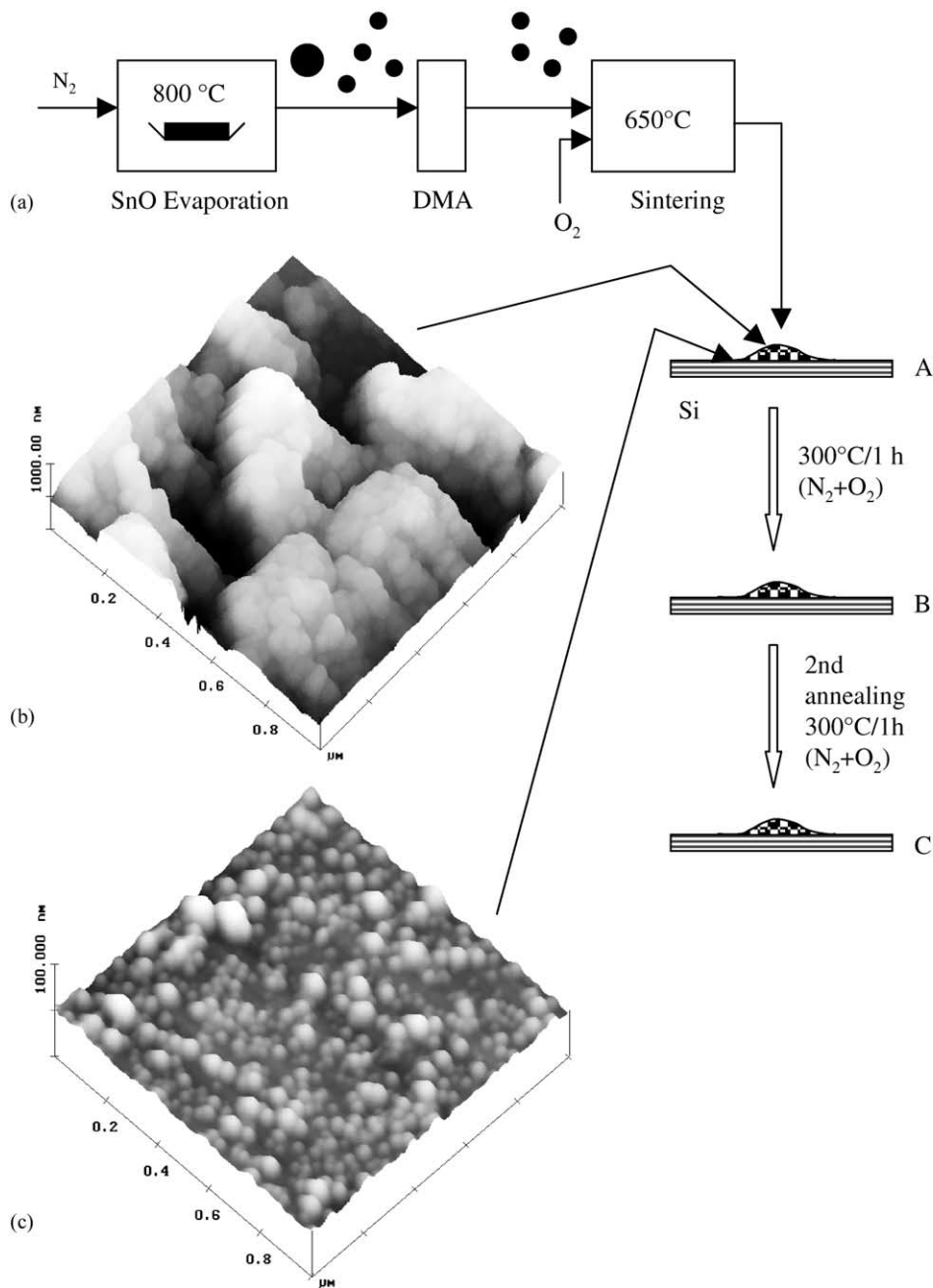


Fig. 1. Schematic diagram of the synthesis setup of nanoparticles (a) and AFM images of 10 nm SnO particles at two different sites of the deposition spot (b) and (c) as indicated by arrows.

inflight oxidation of the SnO particles, oxygen is supplied to the carrier gas flow at concentrations of 10, 20 and 35 vol.% in the sintering stage. The SnO particles are then collected onto a small spot of 1–2 mm in diameter on a Si(1 1 1) substrate in the deposition chamber at room temperature by a low-pressure impaction method. The Si substrate is etched with hydrofluoric acid to remove the native oxide. However, a small amount of oxygen contamination is still observed.

The particle morphology and coverage on different places of the samples are studied by ex situ atomic force microscopy (AFM) (Nanoscope III, Digital Instruments) in non-contact mode. To determine the surface stoichiometry, the samples are transferred under ambient atmosphere to an ultrahigh vacuum chamber for electron-induced AES. The base pressure in the analysis chamber is below  $1 \times 10^{-9}$  hPa. AES spectra are recorded in the first derivative mode and the energy of the primary electron beam is adjusted to 3 keV. The oxygen stoichiometry is estimated from the ratio of the Auger peak-to-peak heights of the O(KLL) line at a kinetic energy of 510 eV and the low-energy feature of the Sn(MNN) doublet at 421 eV. The AES spectrum of sintered SnO<sub>2</sub> powder was used as a calibration reference for determining the oxygen content in the SnO<sub>x</sub> nanoparticles.

Post-annealing of the samples occurs at 300 °C for 1 h in a continuous flow of synthetic air. After AES measurements of those annealed samples, they are once again annealed under the same conditions to study the variation of oxygen stoichiometry due to multiple heat treatments. The post-annealing parameters were chosen to match the working conditions of typical SnO<sub>x</sub> gas sensors.

### 3. Results and discussion

#### 3.1. Morphology

Transmission electron microscopy studies (not shown here) demonstrate that the SnO nanoparticles are spherical and monodisperse when deposited on the Si substrates. AFM images of 10 nm particles at the center and at the edge of the deposition spot are shown in Figs. 1(b) and (c), respectively. In the area of low coverage, Fig. 1(c), individual particles and small clusters of a few particles are observed. In the high coverage regions, large agglomerates of particles up to heights of 300 nm are probed. Obviously, the roughness of the deposited film is increased with larger coverage. Due to a tip size of 20 nm the lateral extension of the imaged particles appears larger than 10 nm. However, the correct diameter of  $(10 \pm 1)$  nm is extracted from the vertical modulation in Fig. 1(c).

#### 3.2. Chemical composition of deposited and post-annealed SnO nanoparticles

The top panel of Fig. 2 shows a typical AES spectrum recorded from 10 nm SnO nanoparticles deposited on a

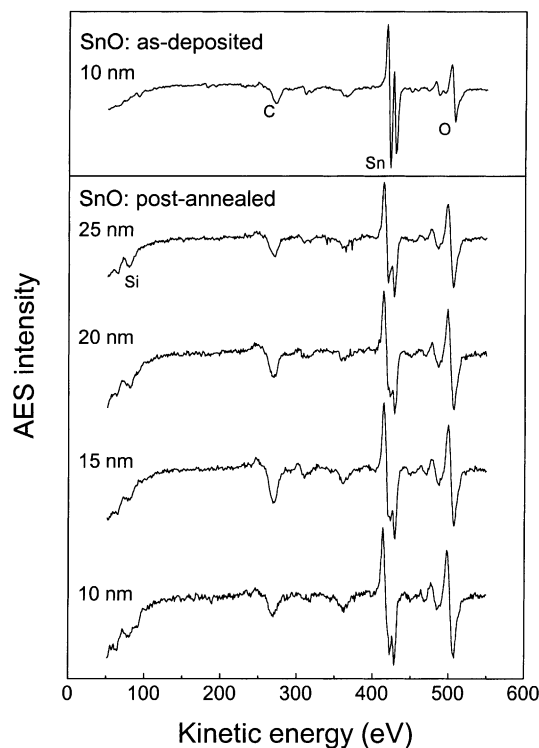


Fig. 2. Upper panel: Auger spectrum of as-deposited 10 nm SnO nanoparticles; lower panel: Auger spectra of SnO nanoparticles of different size annealed once at 300 °C for 1 h in synthetic air.

Si(1 1 1) surface. The Sn(MNN) doublet consists of two well-separated features at 421 and 429 eV. The intensity ratio between the O and Sn Auger features corresponds to a composition of SnO<sub>1.2</sub>. This finding is in agreement with X-ray studies which prove the tetragonal SnO phase of the particles. The C signal at 270 eV is due to residual hydrocarbon contamination during transfer of the samples from the deposition to the analysis chamber. Shape and intensity of the Auger lines do not change with the particle size indicating that the composition is independent of the particle diameter.

The samples are post-annealed at 300 °C for 1 h in synthetic air. Auger spectra of annealed nanoparticles of different sizes are shown in the lower panel of Fig. 2. This treatment changes the shape of the Sn doublet significantly. The double structure in the first derivative spectrum corresponds to a well-resolved double peak structure in the original spectrum which may be retrieved by numerical integration of the recorded Auger spectra. The observed variation of the line shape due to annealing indicates a broadening of the original peaks which may be attributed to different chemical environments of the tin atoms. Similar line distortions were reported earlier for as-deposited and annealed (500 °C) SnO<sub>x</sub> films prepared by ion-beam assisted deposition [11]. The authors interpreted this finding with the presence of metallic Sn at the surface which leads to chemically shifted Auger lines. However, in our study no evidence for metallic Sn could be found. The change of the

Sn Auger lines may be related to an intermediate and not fully relaxed oxidation state of the Sn atoms.

Annealing leads also to a structural change of the nanoparticle film since weak Auger features of oxidized Si are observed at around 80 eV. The film apparently opens up when the nanoparticles are oxidized. Oxidation of SnO is accompanied by a volume reduction of approximately 7% and a change of microstructure has been observed with thin films earlier [8,12].

The change of the Sn line shape and the enhanced oxygen signal due to SiO<sub>2</sub> make a quantitative analysis of the nanoparticle stoichiometry intricate. To get a good estimate, the Auger spectra were corrected by subtracting the SiO<sub>2</sub> background signal (see below) and by comparing the results from the peak-to-peak-intensities with an analysis of the original, i.e. integrated spectra. Both ways of determining the Auger line intensities result in a composition of approximately SnO<sub>2</sub>, i.e. the particles are oxidized by the annealing procedure, however, the distorted line shape indicates a mixed oxidation state.

A second post-annealing process at 300 °C for 1 h in synthetic air leads to a further change of the Auger spectra as shown in the top panel of Fig. 3. The Si substrate signal increased due to an enhanced opening of the nanoparticle

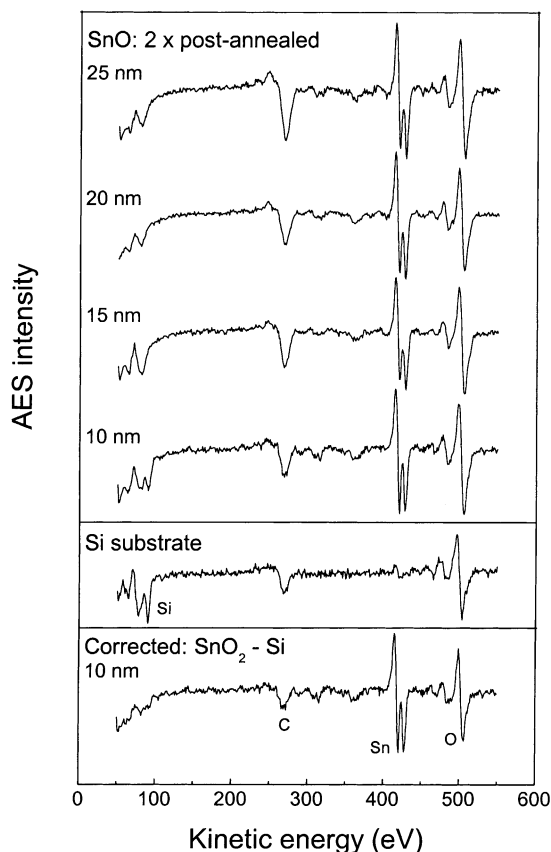


Fig. 3. Upper panel: Auger spectra of SnO<sub>x</sub> nanoparticles of different size post-annealed twice at 300 °C for 1 h in synthetic air; middle panel: Auger spectrum of the Si substrate; lower panel: corrected Auger spectrum for 10 nm SnO<sub>x</sub> nanoparticles.

film. The Sn Auger doublet shows again two well-resolved features indicating a uniform oxidation state. To extract the true stoichiometry of the nanoparticles, the tin oxide spectra are corrected by subtracting the normalized Auger spectrum of the Si substrate shown in the middle panel of Fig. 3. The Si spectrum is normalized to the intensity of the Si line in the tin oxide spectra. The lower panel of Fig. 3 shows the corrected Auger spectrum for the 10 nm nanoparticles as an example. The resulting oxygen content is almost unchanged irrespective of the particle size and corresponds to SnO<sub>1.9</sub>.

### 3.3. Composition of as-deposited and post-annealed, inflight-oxidized SnO<sub>x</sub> nanoparticles

In order to study the properties of nanoparticles oxidized in the gas phase, SnO<sub>x</sub> particles of 20 nm in diameter were prepared by adding 10, 20 and 35 vol.% O<sub>2</sub> into the carrier gas. The increasing oxygen content extracted from the peak-to-peak Auger intensities is plotted as solid squares in Fig. 4. By taking the original Auger line intensities after numerical integration, the error in the determined oxygen content is  $\Delta x \cong \pm 0.2$ . Hence, we can only conclude that with increasing oxygen content in the carrier gas, inflight oxidation of the particles changes the stoichiometry from SnO<sub>1.2</sub> (no O<sub>2</sub>) to SnO<sub>1.8</sub>.

After deposition on the Si substrates the inflight oxidized particles are post-annealed at 300 °C for 1 h in synthetic air. The resulting oxygen contents are also plotted in Fig. 4 for single and double post-annealing steps. The stoichiometry of the nanoparticles is obviously independent of the number of post-annealing steps. All inflight oxidized nanoparticles show a composition of approximately SnO<sub>1.8</sub> which is significantly lower than the oxygen content of post-annealed SnO nanoparticles. Even heating at 300 °C for 4 h in synthetic air does not change the SnO<sub>1.8</sub> composition. Thus, for the given heat treatment, the final stoichiometry of the particles is dependent on its previous history during synthesis. Effective oxidation by post-annealing of the deposited particles is suppressed if the particles are pre-oxidized in the gas phase. A possible explanation may be an inhomogeneous phase mixture of

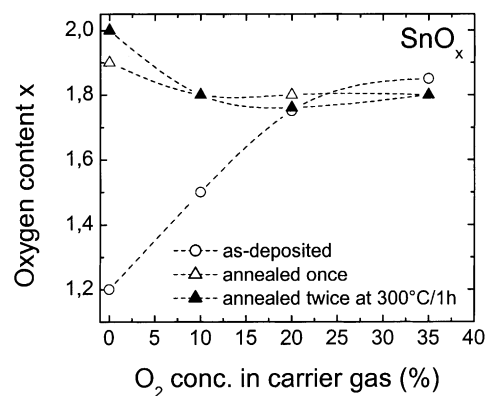


Fig. 4. Change of oxygen content with different concentration of oxygen in the carrier gas before and after annealing. The lines are guides to the eye.

SnO, Sn<sub>3</sub>O<sub>4</sub> and SnO<sub>2</sub> of the inflight oxidized particles. From oxidation studies of thin SnO films, it is known that the transformation into SnO<sub>2</sub> during heating at 500–600 °C for 1 h occurs either directly or by passing an intermediate phase of Sn<sub>3</sub>O<sub>4</sub> [13]. Inflight oxidation occurs on a much shorter time scale (<1 s) and may leave the nanoparticles in a non-uniform state which shows a different oxidation behavior during post-annealing.

#### 4. Conclusions

The oxygen content of SnO nanoparticles oxidized inflight or by a post-annealing process after deposition is independent of the particle size. SnO<sub>x</sub> and SnO nanoparticles prepared with and without oxygen exposure during synthesis behave differently when oxidized after deposition at 300 °C in synthetic air. The SnO particles oxidize into stoichiometric SnO<sub>2</sub> through an intermediate phase of tin oxide revealed by a distorted Auger line shape. On the other hand, the inflight oxidized SnO<sub>x</sub> particles remain in an under-stoichiometric phase of SnO<sub>1.8</sub> even after multiple heat treatments at 300 °C. This may be due to a local, non-uniform oxygen distribution and its internal displacement inhibits the diffusion of external oxygen into the particles in the pre-oxidized cases. Thus, two stabilized phases with different stoichiometry can be obtained. This finding may be of great relevance for the optimization of SnO<sub>x</sub> based gas sensors.

#### Acknowledgements

The support of the Alexander von Humboldt (AvH) Foundation to one of the authors (R.R.) is gratefully acknowledged. The authors thank S. Glass, T. Müller and T.Q. Do for their help during the AES and AFM measurements. Also financial support from the German Science Foundation (DFG) in the

framework of the Collaborative Research Center on ‘Nanoparticles from the gas phase: formation, structure and properties’ (SFB 445) is acknowledged.

#### References

- [1] Y. Shimizu, M. Egashira, Basic aspects and challenges of semiconductor gas sensors, *MRS Bulletin*, June 1999, pp. 18–24.
- [2] C. Xu, J. Tamaki, N. Miura, N. Yamazoe, Grain size effects on gas sensitivity of porous SnO<sub>2</sub>-based elements, *Sens. Actuators, B* 3 (1991) 147–155.
- [3] W. Göpel, K.D. Schierbaum, SnO<sub>2</sub> sensors: current status and future prospects, *Sens. Actuators, B* 26/27 (1995) 1–12.
- [4] B. Flietner, I. Eisele, Work function measurements for gas detection using tin oxide layers with a thickness between 1 and 200 nm, *Thin Solid Films* 250 (1994) 258–262.
- [5] G. Martinelli, M.C. Carotta, E. Traversa, G. Ghiotti, Thick-film gas sensors based on nano-sized semiconducting oxide powders, *MRS Bulletin*, June 1999, pp. 30–36.
- [6] C.L. Lau, G.K. Wertheim, Oxidation of tin: an ESCA study, *J. Vac. Sci. Technol.* 15 (2) (1978) 622–624.
- [7] K.S. Yoo, N.M. Cho, H.S. Song, H.J. Jung, Surface morphology and gas-sensing characteristics of SnO<sub>2-x</sub> thin films oxidized from Sn films, *Sens. Actuators, B* 24/25 (1995) 474–477.
- [8] X.Q. Pan, L. Fu, J.E. Dominquez, Structure-property relationship of nanocrystalline tin dioxide thin films grown on (1012) sapphire, *J. Appl. Phys.* 89 (2001) 6056–6061.
- [9] F.E. Kruis, H. Fissan, Nano-process technology for synthesis and handling of nanoparticles, *KONA Powder Part.* 17 (1999) 130–139.
- [10] M.K. Kennedy, F.E. Kruis, H. Fissan, Gas phase synthesis of size selected SnO<sub>2</sub> nanoparticles for gas sensor applications, *Mater. Sci. Forum* 343/346 (2000) 949–954.
- [11] W.K. Choi, J.S. Cho, S.K. Song, H.J. Jung, S.K. Koh, K.H. Yoon, C.M. Lee, M.C. Sung, K. Jeong, The characterization of undoped SnO<sub>x</sub> thin film grown by reactive ion-assisted deposition, *Thin Solid Films* 304 (1997) 85–97.
- [12] Y.S. Choe, J.H. Chung, D.S. Kim, G.H. Kim, H.K. Baik, Phase transformation and morphological evolution of ion-beam sputtered tin oxide films on silicon substrate, *Mater. Res. Bull.* 34 (1999) 1473–1479.
- [13] J. Geurts, S. Rau, W. Richter, F.J. Schmitte, SnO-films and their oxidation to SnO<sub>2</sub>: Raman scattering, IR-reflectivity and X-ray diffraction study, *Thin Solid Films* 121 (1984) 217–223.